Simultaneous downregulation of uPAR and MMP-9 induces overexpression of the FADD-associated protein RIP and activates caspase 9-mediated apoptosis in gliomas

CHRISTOPHER S. GONDI[1], DZUNG H. DINH[2], MEENA GUJRATI[3] and JASTI S. RAO[1,2]

Departments of [1]Cancer Biology and Pharmacology, [2]Neurosurgery and [3]Pathology,
University of Illinois College of Medicine at Peoria, Peoria, IL, USA

Abstract. We have previously demonstrated the effectiveness of simultaneous RNA interference (RNAi)-mediated down-regulation of urokinase-type plasminogen activator receptor (uPAR) and matrix metalloproteinase-9 (MMP-9) in inhibiting tumor invasion *in vitro* and *in vivo*. In particular, we have shown that the downregulation of uPAR and MMP-9 inhibits intracranial tumor growth. The mechanism of the inhibition of tumor growth has not yet been determined. In this study, we have attempted to explain the mechanisms involved in the inhibition of invasiveness and tumor growth *in vitro*. SNB19 glioma cells were transfected with scrambled vector plasmid (pSV) and a siRNA-expressing plasmid targeting either uPAR (pU) or MMP-9 (pM) singly or in combination (pUM). Untransfected cells were also used as a control. Western blotting and RT-PCR analyses showed the downregulation of uPAR in pU-transfected cells and MMP-9 in pM-transfected cells. In cells transfected with pUM, we observed down-regulation of both uPAR and MMP-9, thereby indicating the specificity of the siRNA-expressing plasmids. An increase in caspase 9 expression was observed in cells transfected with pUM whereas no change in the level of caspase 9 was observed in pU or pM-transfected cells. Additionally, no change in the expression level of caspase 8 was observed. However, an increase in the expression level of cleaved PARP was observed in the case of cells transfected with pU, pM and pUM. Cells transfected with pUM showed the highest levels of cleaved PARP expression. Expression levels of APAF-1 were also higher in pUM-transfected cells with no change in expression levels of controls and in pU and pM-transfected cells. Total CAD expression levels did not change under any of the transfection conditions. However, immunohistochemical studies demonstrated that CAD was translocated to the nucleus, thereby indicating DNA damage. As determined by Western blot analysis of subcellular fractions, cytoplasmic levels of cytochrome c were also increased. We determined the extent of DNA damage using the TUNEL assay (poly-A termination of free -OH ends of degraded nuclear DNA). Based on our results we conclude that the simultaneous downregulation of uPAR and MMP-9 induces apoptosome-mediated apoptosis.

Introduction

Apoptosis (programmed cell death), is a genetically regulated mechanism with a central role in metazoan development and homeostasis. Death receptors (Fas, TNFR-2, DR3 and TRAIL receptors) induce apoptosis upon ligation to cognate ligands or ectopic expression (1,2). The assembly of a death-inducing signaling complex occurs in a hierarchical manner upon receptor activation. The death domain of the receptor binds to the corresponding domain of the adapter molecule FADD, which in turn recruits the zymogen form of death proteases or caspases. Upon activation of caspases and the subsequent increase in concentration, self-activation occurs and triggers the apoptotic pathway. The cytokine tumor necrosis factor (TNF) elicits a wide range of biological responses, including inflammation, cell proliferation, differentiation and apoptosis (2). Although the molecular mechanisms of TNF signaling have largely been elucidated, the principles that regulate survival and death are still unknown. At least four different mechanisms of regulation can be distinguished: i) NF-κB-mediated induction of proteins of the TNF-R complex; ii) NF-κB-independent protection against apoptosis by the TNF-R-associating factor 2 (TRAF2)-mediated recruitment of anti-apoptotic proteins; iii) dual activation of apoptosis and NF-κB by a single molecule and iv) amplification of the death signal by proteolytic inactivation of signaling proteins that are involved in NF-κB activation or cell survival.

The pro-inflammatory cytokine, TNF, exerts its pleiotropic function by binding to two different receptors-TNF-R1 (55 kDa) and TNF-R2 (75 kDa). The two receptors are characterized by the presence of several cysteine repeats in their extracellular domains, whereas their intracellular domains contain no significant homology. Although TNF-R2 can have an important contribution in a number of responses in specific cell types, TNF-induced effects are mediated by TNF-R1 in most cells. The intracellular domain of the latter is characterized by the presence of an 80 amino acid-long death domain (DD), which is responsible for the generation of the cytotoxic death signals as well as the activation of the transcription factor NF-κB. A similar DD is also found in several cytoplasmic signaling proteins including TNF-R-associated DD protein (TRADD) and Fas-associating protein with a death domain (FADD). Triggering of TNF-R1 by TNF leads to clustering of pre-assembled TNF-R complexes and the recruitment of TRADD to TNF-R via a homotypic DD-DD interaction. TNF-induced signaling pathways lead to the activation of NF-κB and apoptosis, bifurcate at the level of TRADD.

Stimulation of TNF-R1 can simultaneously activate at least two signaling pathways within cells (3). One leads to apoptosis while the other counters the death signal and leads to cell survival. When both pathways are activated by TNF, the cell receiving the signal stays alive and multiplies. However, if the balance is somehow shifted to the death pathway, the cell will finally succumb. Despite our increasing knowledge of the signaling proteins that are involved in these signal transduction pathways, the mechanisms that shift the balance to one side or another are still largely unknown. It is clear that the final decision to live or die is at least partially dependent on the expression level of specific proteins.

Materials and methods

Construction of hpRNA expressing plasmid. PCDNA 3 plasmid with a CMV promoter was used in the construction of the hpRNA-expressing vector, as previously described (4) briefly. The following oligos were synthesized: aattCaagtggcaccacca caacaatatataattgttgtggtggtgccacttg for the matrix metallo-proteinase-9 (MMP-9) inverted repeat sequence and gatccTacagcagtggagagcgattatatataataatcgctctccactgctgtag for the urokinase-type plasminogen activator receptor (uPAR) inverted repeat sequence. Both were synthesized for MMP-9 and uPAR. The inverted repeats were laterally symmetrical, making them self-complimentary, with a five-base pair mismatch in the loop region. These five-base pair mismatches aid in the loop formation of the hpRNA. Oligos were heated in a boiling water bath in 6X SSC for 5 min and allowed to self-anneal by slow cooling to room temperature. The resulting annealed oligos were sequentially ligated to pcDNA 3 at the *Eco*R1 site for MMP-9 and *Bam*HI site for uPAR. The resulting plasmid was named pUM. Two single constructs were also made: pU targeting uPAR alone and pM targeting only MMP-9.

Cell culture and transfection. The SNB19 cell line, which was established from a high-grade human glioma, was used in this study. Cells were grown in Dulbecco's modified Eagle's medium/F12 media (1:1, v/v) supplemented with 10% fetal calf serum in a humidified atmosphere containing 5% CO_2 at 37°C. SNB19 cells at 60% confluency in 100-mm tissue culture plates were transfected with 10 μg of siRNA-expressing plasmid constructs (EV/SV, pU, pM or pUM) using lipofectamine as per manufacturer's instructions (Life Technologies, Rockville, MD). Following transfection, conditioned media and cell lysates were assessed for uPAR and MMP-9 expression levels using Western blot analysis and gelatin zymography as per standard protocols.

Western blot analysis. SNB19 cells were transfected with mock, empty vector (EV)/scrambled vector (SV), pM, pU, or pUM. After 48 h, cells were collected and total cell lysates were prepared in standard RIPA extraction buffer containing aprotinin and phenylmethylsulfonyl fluoride. The extracts were incubated at 37°C for 5 min and then centrifuged to separate the lower (detergent) phase, which mainly contains hydrophobic membrane proteins including the glycosyl-phosphatidylinositol-anchored uPAR. Subsequently, 20 μg of protein from these samples were separated under non-reducing conditions by 12% SDS-PAGE and transferred to nitro-cellulose membranes (Schleicher & Schuell, Keene, NH). The membranes were probed for 2 h with antibodies against RIP, cleaved PARP, APAF-1, caspase 8, and caspase 9 as per standard protocols. The membranes were subsequently washed three times with PBS to remove excess primary antibodies, incubated with appropriate HRP-conjugated secondary antibodies and then developed according to enhanced chemiluminescence protocol (Amersham, Arlington Heights, IL). For loading control, the membranes were stripped and probed with monoclonal antibodies for GAPDH as per standard protocol.

Gelatin zymography. PMA-induced MMP-9 expression was analyzed using zymography after transfection of SNB19 cells with EV/SV, pU, pM or pUM. Twenty-four hours after transfection, serum-containing media were replaced with serum-free media and the cells were stimulated with 100 nM PMA. After an additional 24 h incubation period, conditioned media were collected from cells and centrifuged to remove cellular debris. Conditioned media were also collected from untreated cells maintained under similar conditions and analyzed as the control (mock). Equal amounts of protein (30 μg) were subjected to electrophoresis on 10% SDS gels containing gelatin (0.5 mg/ml). Gels were stained with amido black (Sigma Aldrich, St. Louis, MO) and gelatinase activity of MMP-9 was visualized as clear bands on a dark blue background at areas corresponding to the molecular weight of MMP-9 protein.

In situ terminal-deoxytransferase mediated dUTP nick end-labeling (TUNEL) assay. A TUNEL apoptosis detection kit (Upstate Biotechnology Inc, Lake Placid, NY) was used for DNA fragmentation fluorescence staining according to the manufacturer's protocol. Briefly, SNB19 cells, which were grown on chamber slides, were transfected with RNAi constructs targeting uPAR (pU), MMP-9 (pM), uPAR and MMP-9 in combination (pUM), or with empty vector/scrambled vector (EV/SV). Seventy-two hours after

transfection, cells were fixed with 4% paraformaldehyde 0.1 M phosphate buffer (pH 7.4). Then, cells were incubated with a reaction mix containing biotin-dUTP and terminal deoxynucleotidyl transferase for 60 min. Fluorescein-conjugated avidin was applied to the samples, which were then incubated in the dark for 30 min. Positively stained fluorescein-labeled cells were visualized and photographed using fluorescence microscopy.

Immunohistochemistry. SNB19 cells were cultured in 8-well chamber slides at a concentration of $5x10^3$ cells/well. After a 24 h incubation period, cells were transfected with EV/SV, pU, pM or pUM. Untreated cells were also cultured under similar conditions and served as the control. Following an incubation period of 48 h, cells were fixed with 3.7% formaldehyde and then blocked with 1% bovine serum albumin (BSA) for 1 h at room temperature. The slides were then incubated with primary antibody (anti-caspase 9 cleaved) diluted to a concentration of 1:200 in BSA overnight at 4°C. Slides were washed three times with PBS to remove excess primary antibody and cells were then incubated in anti-mouse HRP-conjugated IgG (suitable to primary antibody) at a concentration of 1:500 for 1 h at room temperature. The slides were washed three times with PBS and HPR substrate DAB was added for visualization of caspase 9 expression.

DNA fragmentation assay. SNB19 cells were cultured in 100-mm culture plates at a concentration of $1x10^6$ cells/plate. After a 24 h incubation period, cells were transfected with EV/SV, pU, pM or pUM. Untreated cells were also cultured under similar conditions and served as the control. Genomic DNA was extracted as per standard protocol and electrophoresed on a 0.8% agarose gel using TBE buffer. DNA fragmentation was visualized under UV light after staining with ethidium bromide.

Isolation of mitochondrial and cytosolic cell fractions. SNB19 cells, which were cultured on chamber slides, were transfected with mock, empty vector (EV)/scrambled vector (SV), pU, pM, or pUM and cultured for 48 h. Then, cells were harvested, washed twice in ice-cold distilled water and resuspended in 0.5 g/ml osmotic buffer (10 mM $NaPO_4$, 1.35 M sorbitol, 1 mM EDTA, 2.5 mM dithiothreitol, pH 7.5) with Zymolyase 20T (Seikagaku Corp., E. Falmouth, MA) added to a final concentration of 100 μg/ml. The cells were incubated at 30°C with gentle shaking for 5 min, after which they were resuspended in lysis buffer (0.6 M mannitol, 2 mM EDTA, pH 7.0). Protease inhibitors, PMSF, and aprotinin were added to the lysis buffer immediately prior to cell lysis. Cells were lysed by vigorous vortexing and cellular debris was removed by centrifugation (1,900 x g for 5 min). The supernatant containing both the mitochondrial and cytosolic fractions was then centrifuged (12,100 x g 10 min) to pellet the mitochondria. The resulting supernatant, designated as the cytosolic fraction, was frozen at -80°C or used immediately for Western blotting. The mitochondrial pellet was washed once in 0.6 M mannitol, 2 mM EDTA, pH 7.0, and centrifuged at 1,651 x g for 5 min to pellet any remaining debris. The supernatant containing the mitochondria was then pelleted by centrifugation (23,000 x g for 10 min), resuspended in 10 mM $NaPO_4$ (pH 7.0) for a final

concentration of 5-10 μg/μl and stored at -80°C or used immediately. Intact mitochondria were lysed in lysis buffer (150 mM NaCl, 50 mM Tris-HCl, 2 mM EDTA, 1% NP-40, pH 7.4) and Western blotted. Western blotting for cytochrome c in the cytosolic and mitochondrial fractions was performed as per standard protocol.

Transmission electron microscopy. SNB19 cells, which were grown on chamber slides, were transfected with RNAi constructs targeting uPAR (pU), MMP-9 (pM), uPAR and MMP-9 in combination (pUM), or with empty vector (EV). Seventy-two hours after transfection, the cells were fixed in 10% buffered formaldehyde, immunoprobed for CAD using 5 nm gold-conjugated secondary antibody and processed for electromicroscopy. For transmission electron microscopy, gelatin capsules with LR white were polymerized on the cell surface side of chamber slides. The polymerized gelatin capsules were then processed for transmission electron microscopy.

Results

RNAi-mediated targeting of uPAR and MMP-9 decreases uPAR and MMP-9 mRNA and protein expression levels. uPAR protein expression levels were significantly decreased in pU and pUM-transfected cells as compared to controls, SV-transfected cells and pM-transfected cells (Fig. 1A). MMP-9 enzymatic activity was analyzed in conditioned media collected from control cells as well as from cells treated with pSV, pU, pM and pUM using gelatin zymography (Fig. 1B). MMP-9 activity decreased significantly in the conditioned media collected from pM- and pUM-treated cells when compared to control, pSV- and pU-treated cells. Cells treated with pUM exhibited lower MMP-9 activity than cells treated with pM. However, no change was observed in MMP-2 activity. Quantative analysis reveled that expression levels of uPAR decreased 5-fold in puPAR-treated cells and 10-fold in pUM-treated cells (Fig. 1C). Quantative analysis of levels of MMP-9 expression reveled that MMP-9 expression was reduced in puPAR-treated cells by 1.25-fold whereas cells treated with pMMP-9 decreased by 4.5-fold, in pUM-treated cells levels of MMP-9 decreased by >10-fold (Fig. 1D). RT-PCR analysis of DNA from cells transfected with pU, pM and pUM revealed significant decreases in mRNA levels of uPAR and MMP-9 as compared to the controls (Fig. 1E). The reduction in mRNA level was more significant with pUM transfection as compared to transfection with either of the single constructs. Scrambled vector-treated cells did not have any effect on the mRNA and protein levels. GAPDH levels were analyzed at the mRNA and protein levels to serve as a loading control and no differences were observed.

Downregulation of uPAR and MMP-9 induces pro-apoptotic molecules. Fig. 2A shows that the simultaneous down-regulation of uPAR, MMP-9 singly and simultaneously induced the expression of Receptor-interacting Protein kinase (RIP) and activated cleavage of Poly (ADP-ribose) polymerase (PARP). Increase in apoptotic protease activating factor 1 (APAF-1) expression was observed only in pMMP-9 and pUM-transfected cells, with pUM-transfected cells showing
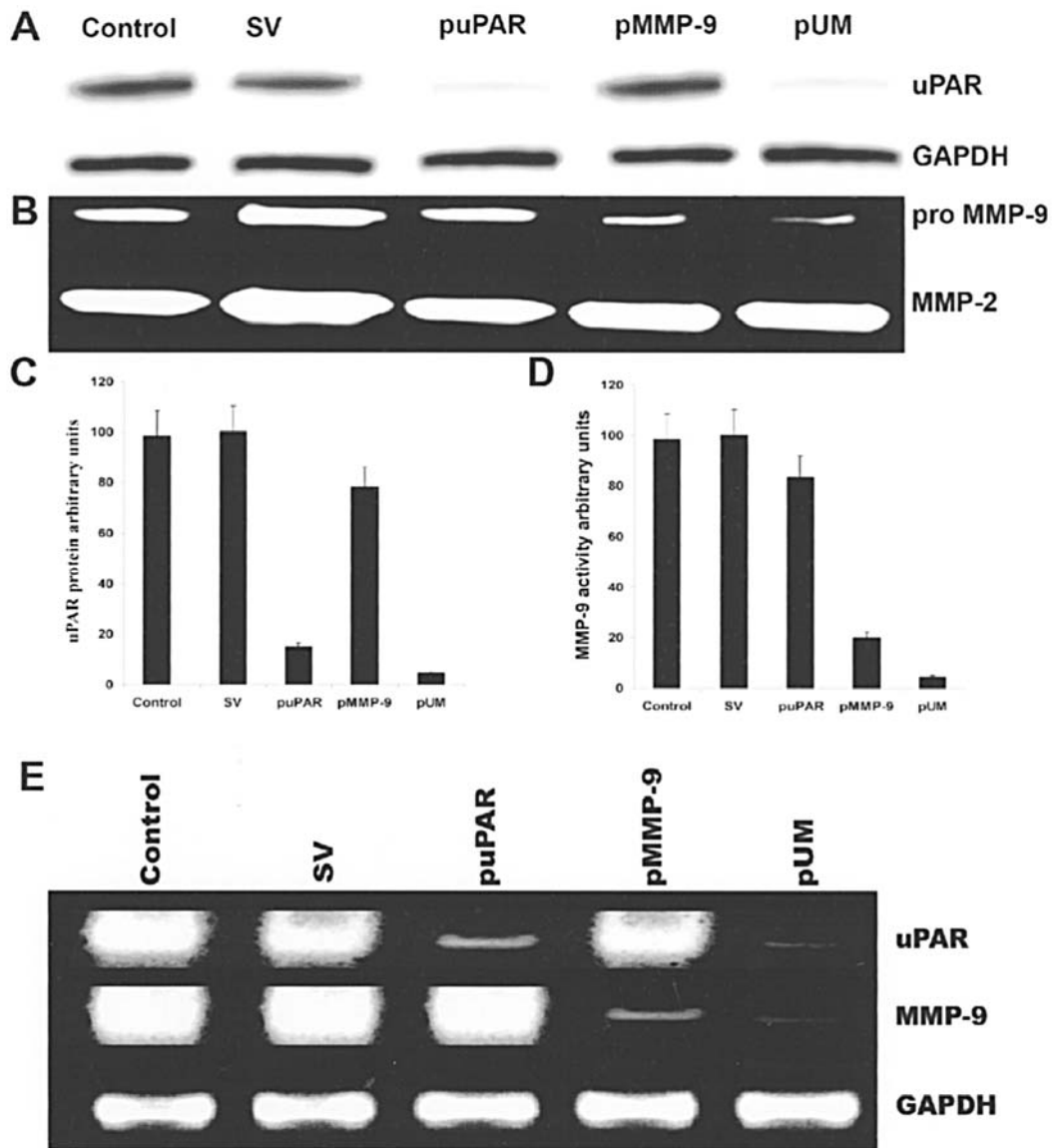
Figure 1. SNB19 cells were transfected with scrambled vector and a vector encoding single or combination siRNA for uPAR and MMP-9 (puPAR, pMMP-9 and pUM). (A) Western blot analysis was performed using an antibody specific for uPAR. GAPDH was simultaneously immunodetected to verify the loading of similar amounts of cell lysates. (B) Conditioned media containing equal amounts of protein (20 μg) from cells transfected with EV/SV, pU, pM and pUM was mixed with sample buffer and run on 10% SDS-PAGE gels containing 0.1% gelatin to determine MMP-9 activity by gelatin zymography. Quantification of uPAR protein (C) and MMP-9 enzymatic activity (D) was obtained by scanning the autoradiograms with densitometry. Data are shown as mean values ± SD of four different experiments from each group (p<0.002). RT-PCR of SNB19 cells transfected with EV/SV, pU, pM and pUM (E). RT-PCR was performed as per standard protocols. Briefly, 72 h after transfection, total RNA was isolated as per standard protocol and first-strand cDNA was synthesized using a cDNA synthesis kit. PCR reaction was set up using the first-strand cDNA as a template for uPAR and MMP-9; PCR for GAPDH was also set up to serve as a loading control.

the highest increase in APAf-1 expression. Activation of caspase 9 but not caspase 8 was observed only in pUM-transfected cells (Fig. 2B) when compared to controls, SV, puPAR or pMMP-9 transfected cells. Genomic DNA electrophoresis demonstrated that cells transfected with pUM exhibited DNA degradation, whereas little DNA damage was observed in cells transfected with pU or pM. Controls SV, puPAR and pMMP-9-transfected cells did not show any DNA damage (Fig. 2C).

Simultaneous downregulation of uPAR and MMP-9 induces nuclear CAD localization and mitochondrial cytochrome c release. Cells transfected with pU and pUM showed CAD localization in the nucleus as determined from transmission electron microscopy studies (Fig. 3A), which indicates DNA

degradation. Western blot analysis of nuclear and cytoplasmic fraction of cells transfected with SV, puPAR, pMMP-9 or pUM was performed and levels of CAD and cytochrome c were determined. Nuclear fraction isolates of the control, SV and pMMP-9-transfected cells did not show the presence of CAD. Nuclear CAD was observed in puPAR and pUM-transfected cells (Fig. 3B). Further, cytoplasmic fractions of cells transfected with puPAR or pUM showed presence of cytoplasmic cytochrome c, which is indicative of mitochondrial permeability (Fig. 3B).

Simultaneous downregulation of uPAR and MMP-9 induces DNA fragmentation as determined by TUNEL assay. Cells transfected with pUM showed TUNEL-positive cells seen as green fluorescence (Fig. 4A). Quantative analysis of TUNEL
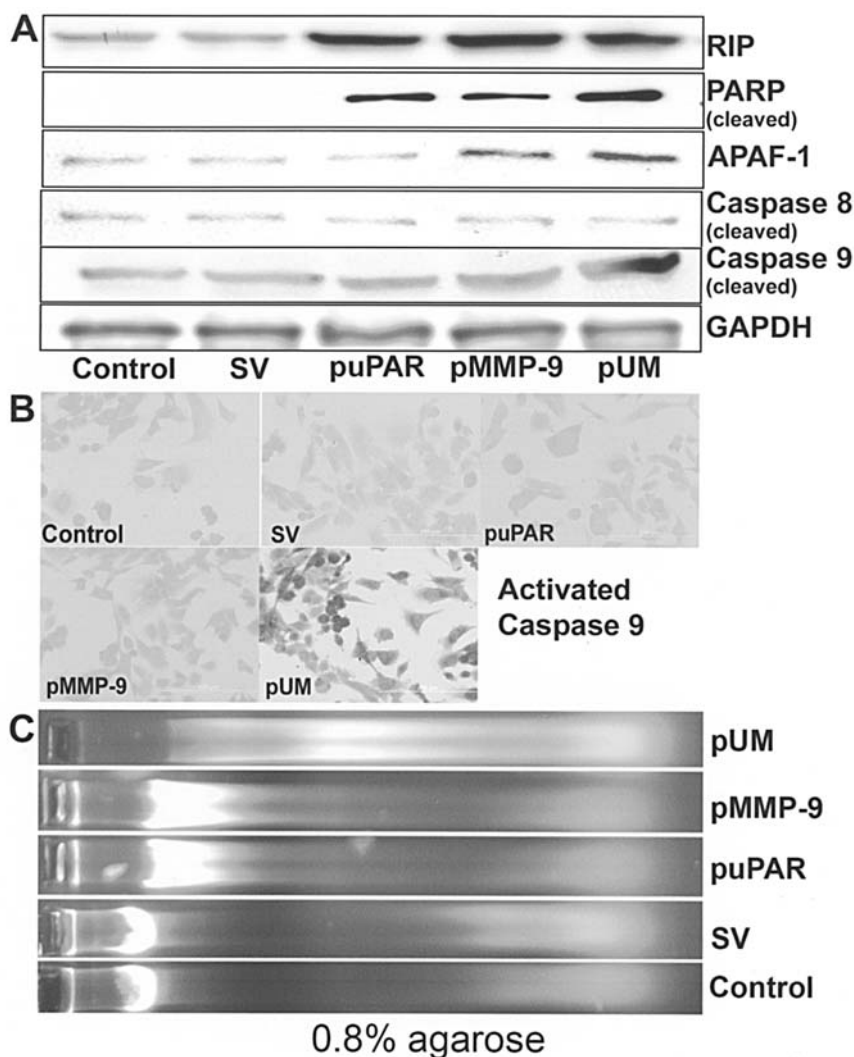
Figure 2. RNAi-mediated downregulation of uPAR and MMP-9 induces RIP and APAF-1 expression, cleavage of PARP and activation of caspase 9. Western blot analysis of total and phosphorylated forms of MAPK, ERK and AKT. SNB19 cells were transfected with EV/SV, pU, pM and pUM. Cells were lysed 72 h later and subjected to SDS-PAGE and immunoblotting for RIP, cleaved PARP, APAF-1, cleaved caspase 8 and cleaved caspase 9 antibodies. GADPH antibodies were used to verify that similar amounts of protein were loaded in each lane (A). SNB19 cells ($1x10^4$) were seeded onto Lab-Tek II chamber slides and transfected with mock, an empty/scrambled vector and a vector encoding single or combination siRNA for uPAR and MMP-9 (pU, pM, pUM). After 72 h, cells were fixed, washed for 1 h with blocking buffer and stained for expression of activated caspase 9 using a specific antibody (B). To determine the status of nuclear material in uPAR- and MMP-9-downregulated SNB19 cells, total nuclear DNA was isolated and electrophoretically separated on a 0.8% agarose gel (C).

assay results indicated that <5% of puPAR and pMMP-9-transfected cells showed fluorescence, whereas cells transfected with pUM showed >75% fluorescence (Fig. 4B).

Discussion

RNA interference (RNAi) is the phenomenon wherein gene expression is effectively suppressed through the introduction of gene-specific, double-stranded RNA (dsRNA). The phenomenon was first observed in plants, later in the worm caenorhabditis and subsequent studies have shown that RNAi exists in a wide variety of eukaryotic organisms including mammals (5,6). RNAi was originally believed to work as a defense mechanism against invading viruses, but preliminary studies have shown that it also has a role in maintenance of heterochromatin during mitosis and meiosis. Once the dsRNA is introduced into a cell, Rnase III cleaves it into double-stranded 21 to 23 nucleotides, called small interfering RNAs (siRNA), in an ATP-dependent manner. These siRNA become

integrated into a multi-subunit protein complex termed RNA-dependent silencing complex (RISC) that guides the siRNA to the target (7). In recent years, RNAi treatment has been shown to have therapeutic benefits in a variety of *in vivo* disease models (8,9).

Cancer progression involves complex mechanisms and depends mainly on the degradation of the extracellular matrix, which is accomplished by various classes of proteinases. Several earlier studies have reported the increased expression of uPAR in various types of cancers (10-12) as well as its localization and active role at the tumor invasion front (13,14). Furthermore, earlier reports suggested a strong role for uPAR in cell adhesion since uPAR consists of a site for binding to vitronectin (15). Several studies also revealed that uPAR initiates intracellular events and thus contributes to cell proliferation (16,17).

Elevated MMP-9 levels have been reported in various cancers (18-21). Studies have reported elevated expression of both uPAR and MMP-9 in human gliomas (22). From our
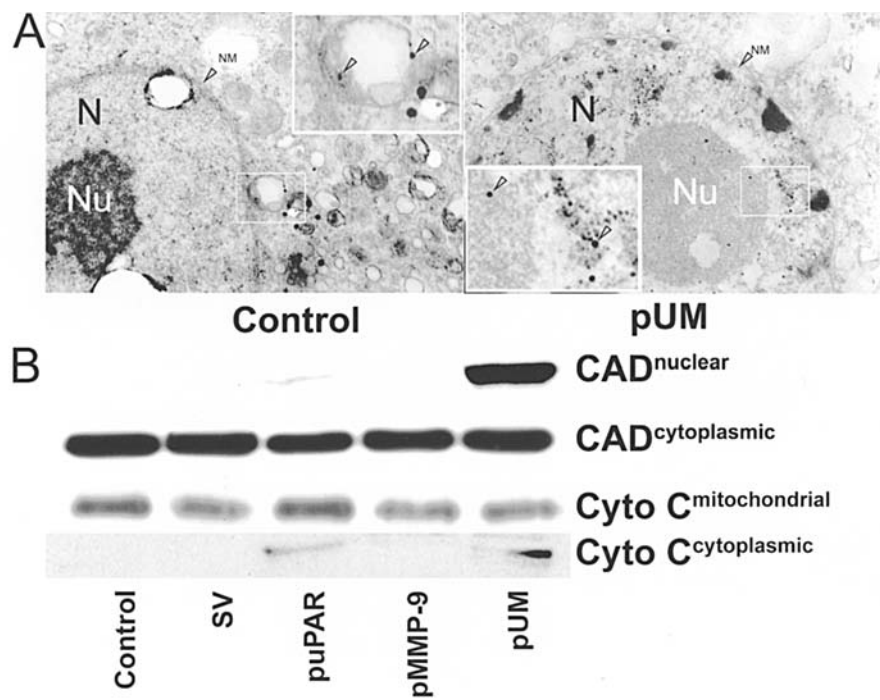
Figure 3. SNB19 cells, which were grown on chamber slides, were transfected with RNAi constructs targeting uPAR (pU), MMP-9 (pM), uPAR and MMP-9 in combination (pUM), or with empty vector (EV). Seventy-two hours after transfection, the cells were fixed in 10% buffered formaldehyde and immunoprobed for CAD using 5 nm gold-conjugated secondary antibody and processed for electromicroscopy. For transmission electron microscopy, gelatin capsules with LR white were polymerized on the cell surface side of chamber slides. The polymerized gelatin capsules were then processed for transmission electron microscopy (A). The subcellular fractions of SNB19 cells transfected with RNAi constructs targeting uPAR (pU), MMP-9 (pM), uPAR and MMP-9 in combination (pUM), or with empty vector (EV) were isolated as per standard protocols 72 h after transfection. Proteins were isolated from the nuclear, mitochondrial and cytoplasmic fractions and an equal quantity of proteins (50 μg) was electrophoresed on SDS gels. The gels were blotted as per standard protocols and immunoprobed for CAD and cytochrome c using appropriate primary and HRP-conjugated secondary antibodies (B). NM, nuclear membrane; N, nucleus; Nu, nucleous.
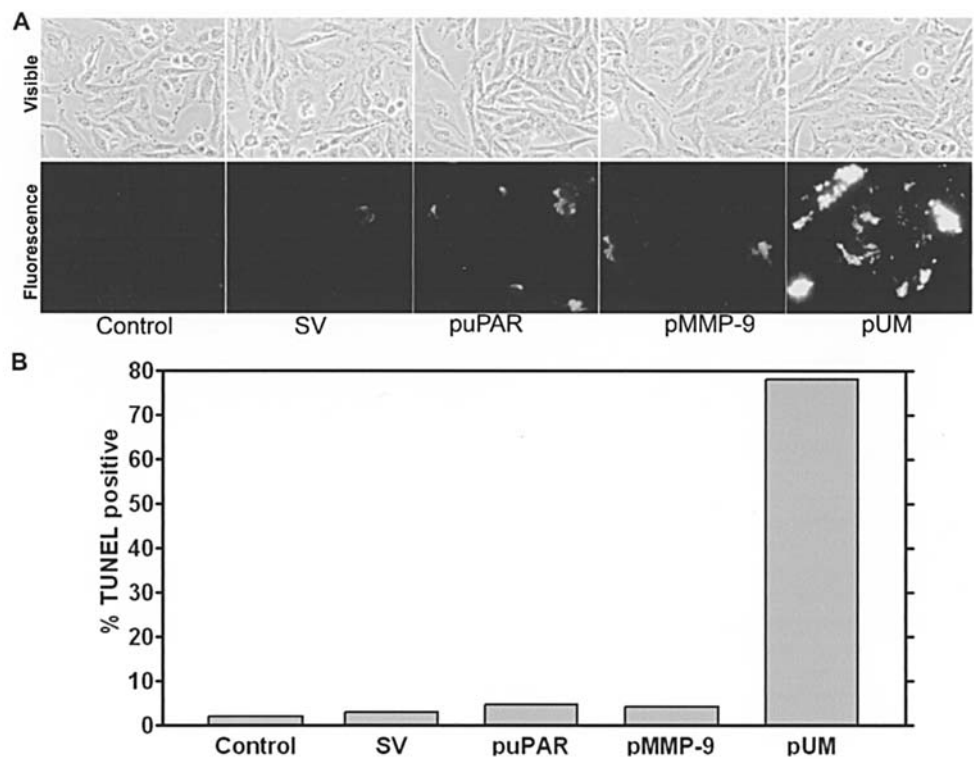

Figure 4. SNB19 cells grown on chamber slides were transfected with RNAi constructs targeting uPAR (pU), MMP-9 (pM), uPAR and MMP-9 in combination (pUM), or with empty vector (EV). Seventy-two hours after transfection, the cells were fixed in paraformaldehyde and processed as per the manufacturer's instructions. Briefly, the TUNEL (Terminal deoxynucleotidyl transferase biotin-dUTP nick end-labeling) method identifies apoptotic cells *in situ* by using terminal deoxynucleotidyl transferase (TdT) to transfer biotin-dUTP to the free 3'-OH of cleaved DNA. The biotin-labeled cleavage sites are then visualized by reaction with fluorescein-conjugated avidin (avidin-FITC). The cells were visualized using a fluorescent microscope with appropriate filter sets. The greatest DNA fragmentation was observed in pUM-transfected cells. Percent apoptosis was calculated based on the amount of fluorescence observed.
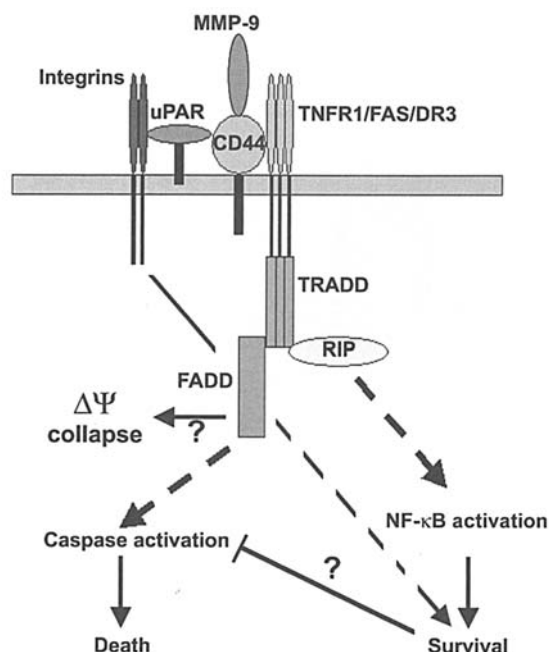
Figure 5. Schematic representation of the involvement of FADD and RIP in the regulation of mitochondrial-mediated apoptosis. RIP initiates a pro-survival pathway whereas FADD activates a pro-apoptotic pathway. This disassociation of RIP from the TRADD complex shifts the balance from survival to death. The inhibitory effect of pro-survival pathways to apoptosis mediated by RIP still remains elusive. The collapse of the mitochondrial membrane potential by FADD remains to be determined.

results, it is evident that RIP levels increased in cells where both uPAR and MMP-9 were downregulated. RIP is known to be associated with TRADD and FADD, which in turn are associated with TNF-α. Several studies have shown that MMPs promote tumor growth, invasion, and metastasis. The increase in secreted MMP-9 activity with TNF-α stimulation in myoblast cells has been observed previously and is due at least in part to an increase in MMP-9 gene transcription. Results showed that an MMP-9 promoter construct was ~5-fold more active in TNF-α-treated myoblasts than in control myoblasts as well as an increase in MMP-9 proteolytic activation, thereby suggesting that MMP activity is a necessary component of growth factor-mediated myoblast migration but also that other consequences of growth factor signaling are necessary for migration to occur (23). Our previous study demonstrating antisense-mediated down-regulation of MMP-9 decreases invasion and migration supports this finding (24) (Fig. 5).

An increase in APAF-1 was also observed in uPAR- and MMP-9-downregulated cells. APAF-1 is known to be involved in the mediation of apoptosis via the apoptosome complex formation (25). It is still not clear what initiates the activation of apoptosome in uPAR- and MMP-9-downregulated cells. Studies of caspases conducted in the past years have elucidated four pathways to caspase activation during apoptosis and can be categorized as: i) the mitochondria-mediated pathway; ii) the death receptor-mediated pathway; iii) the granzyme B-mediated pathway and iv) the endoplasmic reticulum (ER)-mediated pathway. The mitochondrial outer membranes become permeable to proteins, resulting in the release of

proteins normally found in the space between the inner and outer membranes (including cytochrome *c*, apoptosis inducing factor and others). Moreover, the inner mitochondrial membrane's transmembrane potential is reduced (26-28). The release of cytochrome *c* leads to the formation of a heptameric wheel-like caspase-activating complex, which has been termed as an apoptosome. Invariably, the activation of the apoptosome requires ATP and cytochrome c. Our studies have demonstrated that caspase 9 is activated, but not caspase 8, thereby indicating the initiation of the mitochondrial-mediated apoptotic pathway. We reported earlier that the downregulation of uPAR and cathepsin B also initiated apoptosis by activating caspase 8 (rather than caspase 9) with the release of cytochrome c, indicating the initiation of two apoptotic pathways, the mitochondrial and death receptor-mediated pathways (29).

The translocation of CAD from the mitochondria to the nucleus is thought to be associated with nuclear DNA fragmentation, which indicates involvement of the mito-chondrial component. These results demonstrate that uPAR and MMP-9, both being cell surface components, are able to initiate intracellular signaling. However, the mechanisms underlying this cell signaling are not clear. The mechanisms initiating the different signaling pathways, either the activation of caspase 8 or the activation of caspase 9 and the involvement of the mitochondria have yet to be elucidated.

The cleavage of PARP indicates the initiation of nuclear DNA damage, in this case mediated by CAD, which translocates to the nucleus from the mitochondria. CAD nuclear translocation and cytoplasmic cytochrome c were also observed in uPAR-downregulated cells, indicating that the collapse of the mitochondrial membrane potential. In a previous study using antisense-uPAR stable SNB19 cells, mitochondrial membrane potential collapse and activation of caspase 9 were observed; the reason for the differences between our study and the earlier study could be that the previous study used stable cells while we used transiently transfected cells (30).

In the present study, we observed that the downregulation of uPAR alone did cause mitochondrial membrane collapse, but to a much smaller extent when compared to uPAR-MMP-9-downregulated cells. It is probable that over time, uPAR-downregulated cells would induce the activation of caspase 9, though the choice of initiation of caspase 8 or 9 still remains a mystery. In summary, we show that the simultaneous downregulation of uPAR and MMP-9 induces overexpression of RIP and cleavage of PARP. Our study also shows that activated caspase 9 induces nuclear translocation of CAD and induction of DNA degradation as well as a collapse in the mitochondrial membrane potential.

References

1. Henson PM and Hume DA: Apoptotic cell removal in development and tissue homeostasis. Trends Immunol 27: 244-250, 2006.
2. Muzio M: Signalling by proteolysis: death receptors induce apoptosis. Int J Clin Lab Res 28: 141-147, 1998.
3. van Horssen R, Ten Hagen TL and Eggermont AM: TNF-alpha in cancer treatment: molecular insights, antitumor effects, and clinical utility. Oncologist 11: 397-408, 2006.
4. Lakka SS, Gondi CS, Dinh DH, Olivero WC, Gujrati M, Rao VH, Sioka C and Rao JS: Specific interference of uPAR and MMP-9 gene expression induced by double-stranded RNA results in decreased invasion, tumor growth and angiogenesis in gliomas. J Biol Chem 280: 21882-21892, 2005.
5. Fire A, Xu S, Montgomery MK, Kostas SA, Driver SE and Mello CC: Potent and specific genetic interference by double-stranded RNA in Caenorhabditis elegans. Nature 391: 806-811, 1998.
6. Napoli C, Lemieux C and Jorgensen R: Introduction of a chimeric chalcone synthase gene into petunia results in reversible co-suppression of homologous genes in trans. Plant Cell 2: 279-289, 1990.
7. Elbashir SM, Harborth J, Lendeckel W, Yalcin A, Weber K and Tuschl T: Duplexes of 21-nucleotide RNAs mediate RNA interference in cultured mammalian cells. Nature 411: 494-498, 2001.
8. Morris KV, Chan SW, Jacobsen SE and Looney DJ: Small interfering RNA-induced transcriptional gene silencing in human cells. Science 305: 1289-1292, 2004.
9. Soutschek J, Akinc A, Bramlage B, Charisse K, Constien R, Donoghue M, Elbashir S, Geick A, Hadwiger P, Harborth J, John M, Kesavan V, Lavine G, Pandey RK, Racie T, Rajeev KG, Rohl I, Toudjarska I, Wang G, Wuschko S, Bumcrot D, Koteliansky V, Limmer S, Manoharan M and Vornlocher HP: Therapeutic silencing of an endogenous gene by systemic administration of modified siRNAs. Nature 432: 173-178, 2004.
10. Gandhari M, Arens N, Majety M, Dorn-Beineke A and Hildenbrand R: Urokinase-type plasminogen activator induces proliferation in breast cancer cells. Int J Oncol 28: 1463-1470, 2006.
11. Park J, Song SH, Kim TY, Choi MC, Jong HS, Kim TY, Lee JW, Kim NK, Kim WH and Bang YJ: Aberrant methylation of integrin alpha4 gene in human gastric cancer cells. Oncogene 23: 3474-3480, 2004.
12. Zhang L, Zhao ZS, Ru GQ and Ma J: Correlative studies on uPA mRNA and uPAR mRNA expression with vascular endothelial growth factor, microvessel density, progression and survival time of patients with gastric cancer. World J Gastroenterol 12: 3970-3976, 2006.
13. van der Pluijm G, Sijmons B, Vloedgraven H, van der Bent C, Drijfhout JW, Verheijen J, Quax P, Karperien M, Papapoulos S and Lowik C: Urokinase-receptor/integrin complexes are functionally involved in adhesion and progression of human breast cancer in vivo. Am J Pathol 159: 971-982, 2001.
14. Wang XQ, Sun P and Paller AS: Gangliosides inhibit urokinase-type plasminogen activator (uPA)-dependent squamous carcinoma cell migration by preventing uPA receptor/alphabeta integrin/epidermal growth factor receptor interactions. J Invest Dermatol 124: 839-848, 2005.
15. Vial D, Monaghan-Benson E and Keown-Longo PJ: Coordinate regulation of fibronectin matrix assembly by the plasminogen activator system and vitronectin in human osteosarcoma cells. Cancer Cell Int 6: 8, 2006.
16. Adachi Y, Lakka SS, Chandrasekar N, Yanamandra N, Gondi CS, Mohanam S, Dinh DH, Olivero WC, Gujrati M, Tamiya T, Ohmoto T, Kouraklis G, Aggarwal B and Rao JS: Down-regulation of integrin alpha(v)beta(3) expression and integrin-mediated signaling in glioma cells by adenovirus-mediated transfer of antisense urokinase-type plasminogen activator receptor (uPAR) and sense p16 genes. J Biol Chem 276: 47171-47177, 2001.
17. Aguirre-Ghiso JA: Inhibition of FAK signaling activated by urokinase receptor induces dormancy in human carcinoma cells in vivo. Oncogene 21: 2513-2524, 2002.
18. Fernandez CA, Yan L, Louis G, Yang J, Kutok JL and Moses MA: The matrix metalloproteinase-9/neutrophil gelatinase-associated lipocalin complex plays a role in breast tumor growth and is present in the urine of breast cancer patients. Clin Cancer Res 11: 5390-5395, 2005.
19. Gong YL, Xu GM, Huang WD and Chen LB: Expression of matrix metalloproteinases and the tissue inhibitors of metalloproteinases and their local invasiveness and metastasis in Chinese human pancreatic cancer. J Surg Oncol 73: 95-99, 2000.
20. Iizasa T, Fujisawa T, Suzuki M, Motohashi S, Yasufuku K, Yasukawa T, Baba M and Shiba M: Elevated levels of circulating plasma matrix metalloproteinase 9 in non-small cell lung cancer patients. Clin Cancer Res 5: 149-153, 1999.
21. Pereira AM, Strasberg-Rieber M and Rieber M: Invasion-associated MMP-2 and MMP-9 are up-regulated intracellularly in concert with apoptosis linked to melanoma cell detachment. Clin Exp Metastasis 22: 285-295, 2005.
22. Rao JS: Molecular mechanisms of glioma invasiveness: the role of proteases. Nat Rev Cancer 3: 489-501, 2003.
23. Allen DL, Teitelbaum DH and Kurachi K: Growth factor stimulation of matrix metalloproteinase expression and myoblast migration and invasion in vitro. Am J Physiol Cell Physiol 284: C805-C815, 2003.
24. Kondraganti S, Mohanam S, Chintala SK, Kin Y, Jasti SL, Nirmala C, Lakka SS, Adachi Y, Kyritsis AP, Ali-Osman F, Sawaya R, Fuller GN and Rao JS: Selective suppression of matrix metalloproteinase-9 in human glioblastoma cells by antisense gene transfer impairs glioblastoma cell invasion. Cancer Res 60: 6851-6855, 2000.
25. Wang ZB, Liu YQ and Cui YF: Pathways to caspase activation. Cell Biol Int 29: 489-496, 2005.
26. Chang HY and Yang X: Proteases for cell suicide: functions and regulation of caspases. Microbiol Mol Biol Rev 64: 821-846, 2000.
27. Green D and Kroemer G: The central executioners of apoptosis: caspases or mitochondria? Trends Cell Biol 8: 267-271, 1998.
28. Green DR and Reed JC: Mitochondria and apoptosis. Science 281: 1309-1312, 1998.
29. Gondi CS, Kandhukuri N, Kondraganti S, Gujrati M, Olivero WC, Dinh DH and Rao JS: RNA interference-mediated simultaneous down-regulation of urokinase-type plasminogen activator receptor and cathepsin B induces caspase-8-mediated apoptosis in SNB19 human glioma cells. Mol Cancer Ther 5: 3197-3208, 2006.
30. Yanamandra N, Konduri SD, Mohanam S, Dinh DH, Olivero WC, Gujrati M, Nicolson GL, Obeyeseke M and Rao JS: Down-regulation of urokinase-type plasminogen activator receptor (uPAR) induces caspase-mediated cell death in human glioblastoma cells. Clin Exp Metastasis 18: 611-615, 2001.